

# Solar Hydrogen Evolution with Hydrogenases: From Natural to Hybrid Systems

Erwin Reisner<sup>\*[a]</sup>

**Keywords:** Hydrogen / Hydrogenases / Artificial photosynthesis / Electrochemistry / Photochemistry

Natural photosynthesis serves as an inspiration for the development of sustainable fuel-producing systems. Solar energy is utilized to drive redox catalysis energetically uphill, which allows the storage of electromagnetic energy in the chemical bond of a renewable fuel. Hydrogenases are metalloenzymes

that catalyze the reversible reduction of protons to hydrogen at high rates with only minimal driving force. The utilization of hydrogenases for hydrogen production by a range of approaches, from in vivo to artificial hybrid systems, is reviewed.

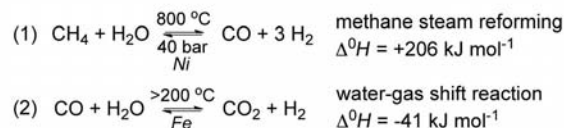
## Introduction

The sun provides us with a continuous and practically inexhaustible flow of energy, and the photochemical conversion of solar to chemical energy in the form of the energy carrier H<sub>2</sub> attracts interest as a replacement for non-renewable fossil fuels.<sup>[1]</sup> Currently, H<sub>2</sub> is produced by the energy-intensive reforming of fossil fuels. Most relevant is the endothermic Ni-catalyzed methane steam reforming of natural gas to synthesis gas [CO/H<sub>2</sub> mixture; Equation (1)] at high temperature and pressure. The slightly exothermic water-gas shift reaction converts CO and H<sub>2</sub>O into fuel-cell grade H<sub>2</sub> and one equivalent of the greenhouse gas CO<sub>2</sub> [Equation (2)].<sup>[2]</sup>

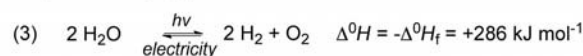
The photolysis of water into its elements, H<sub>2</sub> and O<sub>2</sub>, often referred to as artificial photosynthesis, is an attractive route to produce the solar fuel H<sub>2</sub> [Equation (3)].<sup>[3]</sup> The energy carrier H<sub>2</sub> can then be used either directly as a fuel in fuel cells or be further converted with CO to the liquid fuel methanol<sup>[4]</sup> or to hydrocarbons by Fischer–Tropsch chemistry.<sup>[5]</sup> In addition to the prospect of being used as an energy

carrier in the post-fossil-fuel era, H<sub>2</sub> already has considerable importance for current industrial processes, in particular in the production of ammonia fertilizer (the Haber–Bosch process) and methanol and in petroleum refining.

### Industrial (unsustainable) H<sub>2</sub> production



### Solar (sustainable) H<sub>2</sub> production



### Biological H<sub>2</sub> cycling by [FeFe]- and [NiFe]-hydrogenases



Artificial photosynthetic systems adopt the principles of natural photosynthesis and mimic photobiological energy generation, that is, light harvesting, charge separation, and catalysis (Figure 1).<sup>[6]</sup> An excited photosensitizer (S\*) acts as a low-redox-potential reductant, and a catalytic module uses its low-potential electrons at the electron-acceptor side (C<sup>red</sup>) to carry out reductive chemistry (proton reduction). An electron relay (R) is often needed to transfer the electrons from the photochemical to the catalytic module. The

[a] School of Chemistry, The University of Manchester, Oxford Road, Manchester M13 9PL, UK  
[‡] Current address: Department of Chemistry, University of Cambridge, Lensfield Road, Cambridge CB2 1EW, UK  
E-mail: er376@cam.ac.uk



Erwin Reisner received his degrees from the University of Vienna, Austria (Diploma 2002; PhD 2005 in the group of Bernhard K. Keppler; Habilitation 2010). He worked as an Erwin Schrödinger postdoctoral fellow at the Massachusetts Institute of Technology (Cambridge, MA, USA) in the group of Stephen J. Lippard (2005–2007) and subsequently took up a post as a Research Assistant with Fraser A. Armstrong at the University of Oxford, UK (2008–2009), where he was also active as a College Lecturer (St. John's) in Inorganic Chemistry. After one year as an Engineering and Physical Sciences Research Council (EPSRC) Career Acceleration Fellow at the University of Manchester, UK, he joined the University of Cambridge in October 2010 as a University Lecturer.

necessary electrons can be delivered from the electron donor side by water itself with a potent water oxidation catalyst ( $C^{ox}$ ) to complete the redox cycle. The half-cell donor and acceptor sides are often first studied separately in a sacrificial system (electrons are provided and removed with an external chemical reagent) or by electrochemical methods, but they must then be combined to achieve true water photolysis.

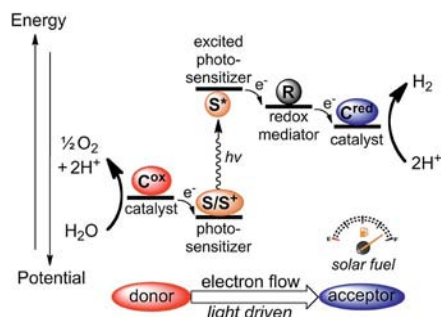


Figure 1. Schematic energy diagram of solar water photolysis. Sunlight ( $h\nu$ ) is absorbed by a photosensitizer (S), resulting in charge separation and transport to deliver reducing and oxidizing equivalents via a redox mediator (R) to an electron acceptor for  $H_2$  production ( $C^{red}$ ) and to an electron donor for water oxidation ( $C^{ox}$ ), respectively.

Selective and economical chemical catalysts are needed for the central chemical conversion of water into  $H_2$  and  $O_2$ .<sup>[7]</sup> Noble metal catalysts such as Pt form  $H_2$  from water with minimal overpotential, but they are severely limited for large-scale production of  $H_2$ . Pt is not only too expensive (limited resources), but also not substrate-specific (at low potentials, Pt is an excellent  $O_2$  reduction catalyst); moreover, it is poisoned by several inhibitors (e.g., CO,  $H_2S$ ). Biology has managed the complex task of catalyzing the cathodic and anodic half reactions of water splitting by using hydrogenases and the oxygen-evolving complex (OEC) of photosystem II (PSII), respectively.<sup>[8]</sup> Here, natural and hybrid solar  $H_2$  production systems utilizing hydrogenases are reviewed.

## Hydrogen Cycling by Hydrogenases

Hydrogenases are widespread metalloenzymes in microorganisms, which utilize  $H_2$  as a reductant to provide low-potential electrons or reduce protons as the final electron acceptor at an unusual organometallic active site.<sup>[9]</sup> The substrates – electrons, protons, and  $H_2$  – are guided separately in well-engineered pathways to and from the active site. Excellent reviews about the structural,<sup>[10]</sup> biological, and physiological role,<sup>[11]</sup> and the spectroscopic<sup>[12]</sup> and electrochemical<sup>[13]</sup> properties of hydrogenases are available.

## Types and Structures of Hydrogenases

Three phylogenetically distinct classes of hydrogenases are known to date. The FeS cluster free [Fe]-hydrogenase is found in some hydrogenotrophic methanogenic archaea,

where it is involved in the pathway that reduces  $CO_2$  to  $CH_4$ .<sup>[14]</sup> [FeFe]-hydrogenases are present in bacteria and some unicellular eukaryotes, and [NiFe]-hydrogenases are found in bacteria and archaea.<sup>[11]</sup> [FeFe]- and [NiFe]-hydrogenases can catalyze the reversible oxidation of  $H_2$  to protons and electrons [Equation (4)], whereas [Fe]-hydrogenase only catalyzes the first step in the uptake reaction – the heterolytic cleavage of  $H_2$ .<sup>[9]</sup> The crystal structure of [Fe]-hydrogenase shows that an octahedral low-spin iron is coordinated in a bidentate fashion to a guanylyl pyridinol cofactor with its  $sp^2$ -hybridized nitrogen and 6-formyl group forming an acyl-iron ligation, a CO, a cysteine, as well as a binding site for an unknown ligand, and a solvent.<sup>[15]</sup> It catalyzes the strictly substrate-dependent reversible reduction of methenyltetrahydromethanopterin with  $H_2$  by hydride transfer at a mononuclear iron active site to methyl-enetetrahydromethanopterin.<sup>[16]</sup>

For the second class, X-ray crystal structures of [FeFe]-hydrogenases from the carbohydrate-fermenting bacterium *Clostridium pasteurianum*,<sup>[17]</sup> the sulfate-reducing bacterium *Desulfovibrio desulfuricans* (Figure 2),<sup>[18]</sup> and the green alga *Chlamydomonas reinhardtii* (HydA<sup>AEFG</sup>) have been determined.<sup>[19]</sup> [FeFe]-hydrogenases are mono- or dimeric enzymes of 45–65 kDa; their usual physiological role is to act as a terminal electron acceptor, which leads to  $H_2$  evolution. The catalytic center is commonly referred to as the H-cluster, which is composed of a ferredoxin-type  $[4Fe-4S]_H$  cluster linked to a  $[2Fe-2S]$  moiety, known as “ $[2Fe]_H$ ”, via a cysteine sulfur atom. Each low-spin iron atom of the  $[2Fe]_H$  cluster is coordinated with one cyanide ( $CN^-$ ) and one or two carbon monoxide groups (CO); the CO molecules sit in hydrophobic pockets, and the  $CN^-$  ligands are involved in hydrogen bonding to the protein.<sup>[20]</sup> The diiron center is bridged by a di- $\mu$ -thiolate, which is either a bis(thiomethyl)amine<sup>[21]</sup> or ether<sup>[17b]</sup> ligand. The bridge-head  $\gamma$ -group presumably acts as a proton shuttle for

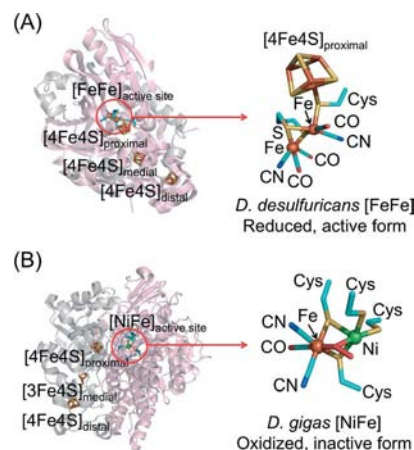


Figure 2. Enzyme ribbon representation and the corresponding active site of (A) *D. desulfuricans* [FeFe]-hydrogenase with protein data bank (PDB) code 1HFE<sup>[18]</sup> in its active form and (B) *Desulfovibrio gigas* [NiFe]-hydrogenase (PDB code 1YQ9)<sup>[23f]</sup> in the oxidized inactive “Ni-A” state; bridging (hydro)peroxido ligand shown in red. The small subunit is depicted in gray and the large subunit in purple.

the active site. The number of FeS clusters other than the H-cluster varies widely in [FeFe]-hydrogenases. Prokaryotic [FeFe]-hydrogenases use a “wire” of up to four FeS clusters, the gram-positive anaerobic bacterium *C. pasteurianum* [FeFe]-hydrogenase I is an example of an enzyme that uses four sites for intraprotein electron transfer to and from the H-cluster active site.<sup>[17a]</sup> In contrast, algal hydrogenases lack this accessory subdomain in the unicellular green alga *Scenedesmus obliquus* HydA and the smallest [FeFe]-hydrogenase, *C. reinhardtii* HydA1.<sup>[19,22]</sup>

In the third class of hydrogenases, crystal structures for several periplasmic [NiFe]-enzymes from sulfate-reducing bacteria (Figure 2)<sup>[23]</sup> and a preliminary structure of the membrane-bound hydrogenase from the photosynthetic purple sulfur bacterium *Allochromatium vinosum*<sup>[24]</sup> are available. The active site in these hydrogenases is embedded in the large subunit with two terminal and two bridging cysteine molecules coordinated to the Ni center, leaving two *cis* coordination sites available for substrate binding in the reduced, active form of the enzyme. Terminal CO and CN<sup>−</sup> ligands, in addition to the cysteine bridges, surround the Fe ion active site. FeS clusters in the small subunit facilitate intraprotein electron translocation, and the proximal [4Fe4S] cluster is located within 14 Å of the active site.<sup>[23]</sup> Crystallographic analysis of *Desulfovibrio fructosovorans* [NiFe]-hydrogenase in a Xe atmosphere and molecular dynamics simulations identified hydrophobic tunnels for gas transport,<sup>[23b]</sup> and gas-transport kinetics were studied experimentally by electrochemical methods.<sup>[25]</sup>

## Hydrogenases as Catalysts

Hydrogenases show high catalytic currents when adsorbed on an electrode surface, and for most enzymes the current trace cuts the zero-current line cleanly at the thermodynamic potential of the H<sup>+</sup>/H<sub>2</sub> couple (Figure 3).<sup>[26]</sup> Thus, most hydrogenases operate reversibly and require only a minimal overpotential to work in either di-

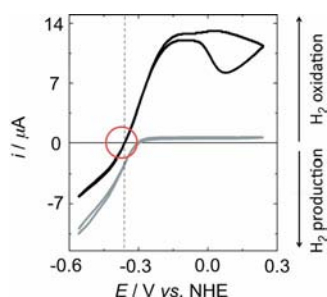


Figure 3. Protein film voltammogram of *D. desulfuricans* [FeFe]-hydrogenase adsorbed on a pyrolytic graphite edge (PGE) electrode. The current (activity of the enzyme) is plotted as a function of potential under Ar (gray line) and H<sub>2</sub> (black line). Negative currents correspond to proton reduction and positive currents to H<sub>2</sub> oxidation. The red circle indicates the sharp cut through zero-current; only a minimal driving force is needed for reversible redox catalysis. Experiments were conducted at 10 °C, pH 6.0, a scan rate of 50 mV s<sup>−1</sup> and an electrode rotation rate of 2500 rpm. Adapted with permission of the Royal Society of Chemistry from ref.<sup>[28]</sup>

rection. The turnover frequency for H<sub>2</sub> oxidation was estimated electrochemically to reach approximately  $5 \times 10^4 \text{ s}^{-1}$ .<sup>[27]</sup> Some hydrogenases also operate with high efficiency in the presence of conventional Pt inhibitors such as CO and H<sub>2</sub>S.<sup>[13]</sup>

Different hydrogenases have distinct properties and are selected for their suitability as enzyme H<sub>2</sub> production catalysts according to the following selection criteria: the enzyme must (1) be a good H<sub>2</sub> producer, (2) not be strongly inhibited by its product, H<sub>2</sub>, and (3) operate in the presence of O<sub>2</sub>.<sup>[28]</sup> The ability of a hydrogenase to operate in the presence of O<sub>2</sub> is not only a prerequisite for a catalyst for the combustion of H<sub>2</sub> and O<sub>2</sub> in an enzyme fuel cell,<sup>[29]</sup> but also a necessary attribute for enzyme-catalyzed production of H<sub>2</sub>, where some O<sub>2</sub> is present from air or is produced as a by-product from water splitting.

[NiFe]-hydrogenases generally show improved robustness towards O<sub>2</sub> than the O<sub>2</sub>-sensitive [FeFe]-hydrogenases. However, the former are traditionally also known for being biased towards H<sub>2</sub> oxidation rather than proton reduction, and H<sub>2</sub> production by [NiFe]-hydrogenases is normally strongly inhibited by H<sub>2</sub>.<sup>[10]</sup> An O<sub>2</sub>-tolerant hydrogenase shows a slow reactivity with O<sub>2</sub> and/or fast reactivation rates upon aerobic inactivation.<sup>[28]</sup> Slow access of O<sub>2</sub> may also help protect some hydrogenases from O<sub>2</sub>. Recovery from an inactive state involves the thermodynamics and kinetics of reductive reactivation.<sup>[30]</sup>

Aerobic inactive states in [NiFe]-hydrogenases are usually due to the formation of paramagnetic Ni<sup>III</sup> species, and either an *unready* Ni-A state (O<sub>2</sub> partially reduced by two electrons; presumably bridging hydroperoxido species) or a *ready* Ni-B state (O<sub>2</sub> fully reduced by four electrons; bridging hydroxide and water elimination) is formed.<sup>[31]</sup> The ratio of these Ni<sup>III</sup> forms depends upon the conditions, in particular on the availability of electrons (redox potential), and is highly hydrogenase-specific.<sup>[32]</sup> Fast reactivation only occurs with the *ready* Ni-B state, whereas reactivation from the *unready* Ni-A state is very slow, making the enzyme unsuitable to operate in the presence of O<sub>2</sub>.<sup>[28]</sup> The formation of unready states may be delayed or prevented by (1) increasing the redox potential of the proximal FeS cluster as suggested for certain membrane-bound [NiFe]-hydrogenases,<sup>[33]</sup> (2) by substituting a cysteine ligand of the Ni by a selenocysteine (see below), or (3) by decreasing the reactivity towards O<sub>2</sub> through changes in the immediate active site environment or mutating residues located in the gas tunnel to the [NiFe]-site.<sup>[25b,34]</sup>

## Intermolecular Electron Transfer

Electron transfer between the distal FeS cluster of a hydrogenase and an electron donor/acceptor is of particular relevance for the construction of artificial photosynthetic systems. The natural redox partner of a hydrogenase depends on its function and location inside the cell.<sup>[35]</sup> The physiological role of a periplasmic hydrogenase is typically to derive reducing equivalents from H<sub>2</sub> as an “uptake” hy-



drogenase. Electrons derived from the  $H_2$  metabolism are used, either directly or indirectly, to reduce  $NAD(P)^+$  via the quinone pool. The protons create a transmembrane proton gradient that is thought to be coupled to ATP synthesis in the cytoplasm.<sup>[20]</sup> Soluble periplasmic  $H_2$  uptake hydrogenases transfer the electrons via a c-type cytochrome (Cyt-c) to the cytoplasmic side of the membrane,<sup>[36]</sup> whilst membrane-bound periplasmic hydrogenases commonly bind to Cyt-b to provide electrons to the quinone pool.

[FeFe]-hydrogenases of green algae and cyanobacterial membrane-bound energy-converting [NiFe]-hydrogenases receive an excess of low-potential electrons at the end of the photosynthetic electron transfer chain and exchange electrons with ferredoxin to use protons as electron acceptors and generate  $H_2$ .<sup>[10]</sup> Algal [FeFe]-hydrogenases, for example, from *C. reinhardtii* [FeFe]-HydA, have an overall negatively charged surface, but leave a positively charged electrostatic surface binding niche for the negatively charged electron donor of the photosynthetic electron transfer ferredoxin (PetF).<sup>[37]</sup> On the other hand, a negative site is observed at the electron-entry site of [NiFe]-hydrogenase (Figure 4), complementary to the positively charged patches on soluble Cyt-c.<sup>[23d]</sup>

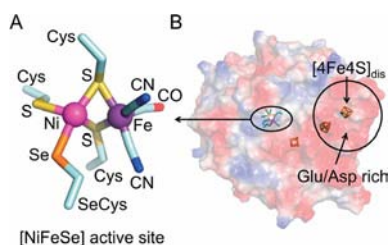


Figure 4. *Desulfomicrobium baculatum* [NiFeSe]-hydrogenase (PDB code 1CC1):<sup>[23c]</sup> (A) reduced active site and (B) looking down the electron-transfer relay into the enzyme from the distal cluster. The surface charge was modeled with a simple vacuum electrostatic model in Pymol; color-coding: red: negative, blue: positive electrostatic charge. The glutamate- and aspartate-rich surface environment around the distal FeS cluster is a common feature for periplasmic [NiFe]-hydrogenases.

### Specific Properties of Selected Hydrogenases

The location and function of a hydrogenase in the cell reflects the enzyme's properties and bias towards  $H_2$  production or oxidation. [FeFe]-hydrogenases are appealing  $H_2$  production catalysts, because they have a higher catalytic activity for  $H_2$  evolution than their [NiFe]-analogues. However, irreversible inhibition and degradation of [FeFe]-hydrogenases by  $O_2$  is a major bottleneck in their utilization.<sup>[38]</sup> Much attention is currently focused on the cytoplasmic [FeFe]-hydrogenase from bacterial *C. pasteurianum* I,<sup>[17a]</sup> algal *C. reinhardtii* [FeFe]-HydA1,<sup>[39]</sup> and bacterial *C. acetobutylicum* [FeFe]-HydA.<sup>[40]</sup>

Unlike algal [FeFe]-hydrogenases, [NiFe]-hydrogenases are reversibly inhibited by  $O_2$ , and some of them can even perform catalysis in the presence of  $O_2$ . Three prototypical [NiFe]-hydrogenases are found in the aerobic Knallgas bacterium *Ralstonia eutropha* H16, which act in the presence of

$O_2$  both in vivo and as isolated enzymes:<sup>[41]</sup> the periplasmic membrane-bound hydrogenase (MBH) and cytoplasmic soluble hydrogenase (SH) are uptake hydrogenases, and a regulatory hydrogenase (RH) acts as a  $H_2$  sensor in a signal transduction pathway, which controls hydrogenase gene expression.<sup>[33]</sup> *R. eutropha* [NiFe]-MBH is remarkably robust towards  $O_2$ .<sup>[33]</sup> Adsorbed on a pyrolytic graphite edge (PGE) electrode, it was used as the anode in a membraneless enzyme hydrogen fuel cell coupled with an  $O_2$ -reducing cathode coated with laccase or bilirubin oxidase (Cu oxidase).<sup>[29]</sup> Although the X-ray crystal structure of *R. eutropha* [NiFe]-MBH remains elusive, much information on its biosynthesis, overproduction, and biochemical properties is available, and it is also accessible to genetic engineering.<sup>[33]</sup> Unfortunately,  $H_2$  evolution in *R. eutropha* [NiFe]-MBH is strongly product-inhibited, limiting its suitability as  $H_2$  evolution catalyst.<sup>[42]</sup>

Membrane-bound [NiFe]-hydrogenase I from the thermophilic bacterium *Aquifex aeolicus*<sup>[43]</sup> oxidizes  $H_2$  with high turnover at elevated temperatures in the presence of  $O_2$  and CO. As for *R. eutropha* [NiFe]-MBH, the "unready" Ni-A state is not observed upon exposure to  $O_2$ ;<sup>[44]</sup> this is a notable common feature of  $O_2$ -tolerant [NiFe]-hydrogenases.<sup>[30]</sup> Three [NiFe]-hydrogenases are expressed in the enterobacterium *Escherichia coli*. The membrane-bound  $H_2$  uptake enzymes *E. coli* [NiFe]-MBHyd1 and MBHyd2 are both located in the periplasm. Electrochemical studies have shown that Hyd1 is active for  $H_2$  oxidation, but it does not operate in the reverse direction, whereas Hyd2 can operate as a bidirectional hydrogenase.<sup>[45]</sup> Hyd1 oxidizes  $H_2$  even in the presence of air, whereas MBHyd2 is  $O_2$ -sensitive at high potential and does not oxidize  $H_2$  under aerobic conditions.<sup>[45]</sup> Cytoplasmic *E. coli* [NiFe]-Hyd3 is responsible for  $H_2$  evolution under fermentative conditions.<sup>[46]</sup> *E. coli* [NiFe]-MBHyd1 attached to a PGE electrode was employed as the anode in an enzyme fuel cell,<sup>[29d]</sup> and *A. aeolicus* [NiFe]-MBH also appears to be a suitable candidate.<sup>[47]</sup>

[NiFeSe]-hydrogenases are a subclass of [NiFe]-hydrogenases that contain a selenocysteine instead of cysteine coordinated to the Ni site (Figure 4) and contain a third [4Fe4S] cluster instead of the medial [3Fe4S] cluster in common [NiFe]-hydrogenases.<sup>[23c]</sup> Examples are the [NiFeSe]-hydrogenases from the sulfate reducing bacteria *Desulfomicrobium baculatum* and *Desulfovibrio vulgaris* Hildenborough, in which the replacement of a sulfur by a selenium appears to cause an improved catalytic function towards  $H_2$  production.<sup>[48]</sup> *D. baculatum* [NiFeSe]-hydrogenase is reactivated from  $O_2$  inactivation at low potential under anaerobic conditions and operates in the presence of small amounts ( $< 1\%$ ) of  $O_2$  at low potential (Figure 5).<sup>[49]</sup> Aerobic treatment of *D. vulgaris* Hildenborough and *D. baculatum* [NiFeSe]-hydrogenase<sup>[50]</sup> results in EPR-silent states with diamagnetic  $Ni^{2+}$ ,<sup>[51]</sup> and the absence of a bridging ligand was identified by X-ray crystallography in the oxidized as-isolated state.<sup>[52]</sup> The fast inhibition of [NiFeSe]-hydrogenase activity by  $O_2$  and its fast reactivation under reducing conditions was explained by oxidation of the terminal ligand of the active site Ni, instead of the direct at-

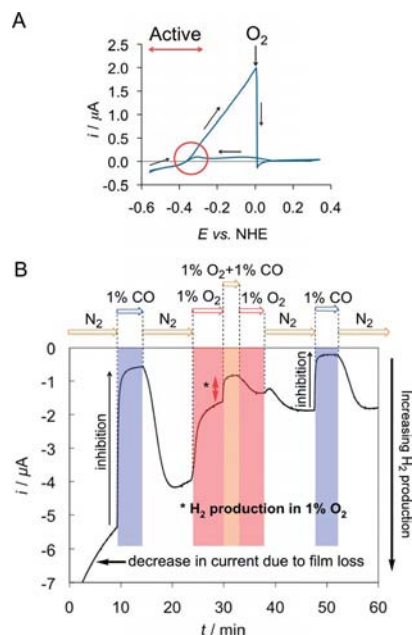


Figure 5. (A) Protein film voltammogram ( $1 \text{ mV s}^{-1}$ ) of the enzyme adsorbed on a rotating-disc PGE electrode at pH 6 at  $25^\circ\text{C}$  under 1 bar  $\text{H}_2$ . At 0 mV vs. NHE on the positive direction scan,  $\text{O}_2$ -saturated buffer was injected and then removed by flushing the headspace in the electrochemical cell with  $\text{H}_2$ . The circle indicates that full reactivation of the  $\text{O}_2$ -inactivated enzyme occurs on the return scan just before the thermodynamic  $\text{H}^+/\text{H}_2$  redox potential. (B) Chrono-amperometric experiment at pH 6 and  $30^\circ\text{C}$ . The enzyme was poised at low potential ( $-0.45 \text{ V}$  vs. NHE) under changing atmospheres of  $\text{N}_2$ , 1% CO in  $\text{N}_2$ , 1%  $\text{O}_2$  in  $\text{N}_2$ , and 1%  $\text{O}_2 + 1\%$  CO in  $\text{N}_2$  as indicated on top of the plot. An exponential current loss results from film loss. Adapted with permission of the American Chemical Society from ref.<sup>[49]</sup>

tachment of  $\text{O}_2$  to the bridging site between Ni and Fe.<sup>[52]</sup> Thus, the molecular details of the aerobic inactivation pathway are distinct from those in common [NiFe]-hydrogenases, where Ni-A and Ni-B states are observed in the oxidized forms. [NiFeSe]-hydrogenase becomes the major hydrogenase expressed by *D. vulgaris* Hildenborough when selenium is available, which leads to a down-regulation of the [NiFe]- and [FeFe]-hydrogenases.<sup>[50]</sup>

## Solar Hydrogen Evolution

Oxygenic organisms use solar energy in two separate light-driven steps in photosystem I (PSI)<sup>[53]</sup> and PSII<sup>[54]</sup> for energetically uphill oxidation/reduction processes during natural photosynthesis. The source of electrons is water, which is photo-oxidized at the OEC to produce  $\text{O}_2$ . The electrons extracted from water are shuttled from PSII along the photosynthetic electron-transport chain and PSI to a freely diffusing ferredoxin;<sup>[55]</sup> the dissociation constant ( $K_d$  value) of a PSI-ferredoxin complex from the cyanobacterial *Synechocystis* sp. strain PCC 6803 was determined to be  $0.14\text{--}0.38 \mu\text{M}$  by backscattering interferometry.<sup>[56]</sup> Ferredoxin usually transfers electrons to a ferredoxin-NADP-oxidoreductase (FNR) that reduces  $\text{NADP}^+$  to NADPH, an electron source for the reduction of  $\text{CO}_2$  to carbohydrates in the Calvin cycle (Figure 6).<sup>[55]</sup>

## $\text{H}_2$ Evolution by Natural Photosynthesis

The energy-converting photosynthetic machinery can be utilized under special conditions for photobiological  $\text{H}_2$  production either through oxygenic photosynthesis by some

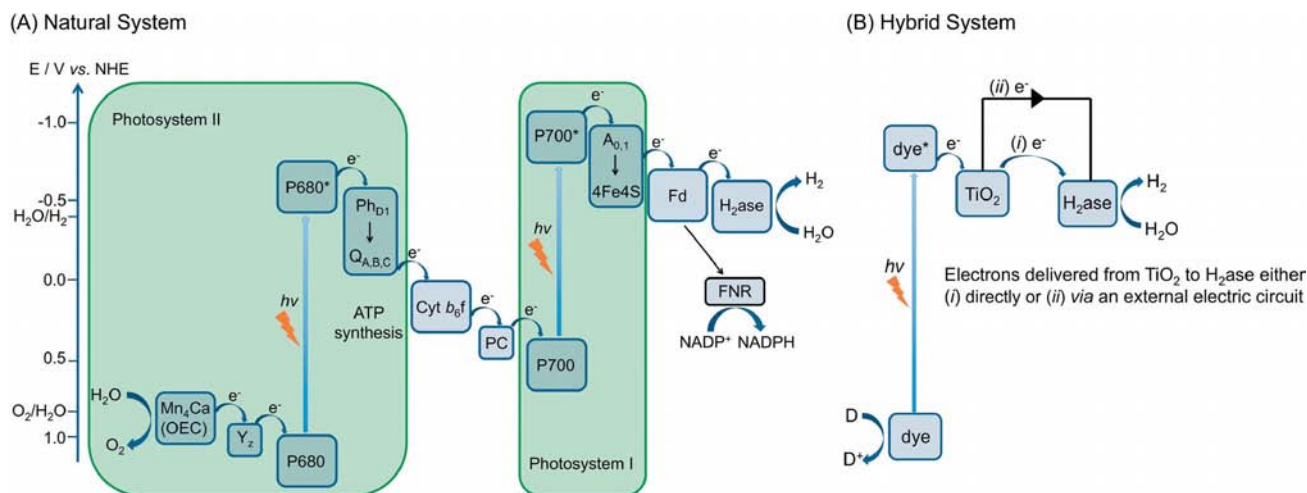


Figure 6. (A) Energy diagram for oxygenic photosynthesis in green algae linked to  $\text{H}_2$  production by a [FeFe]-hydrogenase. Electrons originate either from the oxidation of water at the OEC of PSII or from the oxidation of endogenous cellular substrates. Chlorophylls P680 and P700 act as reaction centers for the absorption of light. Electron transport components are the PSII tyrosine residue ( $\text{Y}_Z$ ), pheophytin (Ph), the terminal PSII electron acceptor plastoquinone (Q), cytochrome  $b_6f$ , plastocyanin (PC), electron acceptors A, and a [4Fe4S] cluster; ferredoxin (Fd) acts as the physiological electron mediator to the hydrogenase ( $\text{H}_2\text{ase}$ ). The competing reduction of  $\text{NADP}^+$  via FNR is also shown (see text). (B) Hybrid hydrogenase-based  $\text{H}_2$  production system. Upon excitation by visible light in the presence of a sacrificial electron donor D, a synthetic dye injects an electron into the conduction band of  $\text{TiO}_2$ . The electrons are transferred either (i) directly to the hydrogenase attached to the metal oxide nanoparticle,<sup>[103]</sup> or (ii) via an external circuit to a hydrogenase attached to a cathode in a photoelectrochemical enzyme fuel cell.<sup>[80]</sup>

green algae and cyanobacteria, or through non-oxygenic photosynthesis in purple photosynthetic bacteria.<sup>[57]</sup> Prototypical  $\text{H}_2$  production occurs in algal *C. reinhardtii*, where [FeFe]-HydA1 catalyzes the evolution of small amounts of  $\text{H}_2$  from the photolysis of water shortly after light shines on dark anaerobic algal cultures. Thereby, protons serve as the electron sink, and electrons are derived from the short-lived reoxidation of the photosynthetic electron-transport chain from PSII and PSI to ferredoxin,<sup>[37a,58]</sup> producing a transient  $\text{H}_2$  burst.<sup>[59]</sup>

$\text{H}_2$  production in photosynthetic oxygenic microorganisms faces major limitations, some of which are: (1)  $\text{O}_2$ -dependent down-regulation and  $\text{O}_2$  sensitivity of hydrogenases, (2) competitive use of photosynthesis-generated reducing equivalents by other physiological functions, and (3) low light saturation properties of algal photosynthesis due to the large chlorophyll antenna system. Algal [FeFe]-hydrogenases are not only  $\text{O}_2$ -sensitive, but they are also only expressed in the absence of  $\text{O}_2$ . In addition, atmospheric  $\text{CO}_2$  is ultimately the preferred terminal electron acceptor, even in the presence of an active hydrogenase. A solar conversion efficiency of five to ten percent was demonstrated in vivo with *C. reinhardtii* under low light intensities (to avoid limitations by light saturation) and by keeping very low partial pressures of  $\text{O}_2$  and  $\text{CO}_2$  by purging the reactor with an inert gas (Figure 6).<sup>[37a,60]</sup>

Sustained photobiological  $\text{H}_2$  production in green algae can be achieved by separating  $\text{H}_2$  production from  $\text{O}_2$  evolution activity by inhibition of the photosynthetic apparatus. One example is the growth of *C. reinhardtii* cultures deprived of sulfur, which results in the reversible inhibition of their photosynthetic activity due to nutrient stress, whilst mitochondrial respiration is left essentially unchanged. The diminished photosynthetic activity is due to down-regulation of the catalytically active D1 subunit of PSII and results in a decline in light-driven water oxidation.<sup>[61]</sup> Once respiration consumes more  $\text{O}_2$  than residual photosynthesis can deliver, cells become anaerobic and induce the reversible hydrogenase pathway of electron transport, allowing for sustained photosynthetic production of  $\text{H}_2$ .<sup>[62]</sup> The reduction of protons is induced, because it is used by the cell as a sink for (excess) electrons that result from endogenous substrate (starch and protein) breakdown.<sup>[59,61,63]</sup>

## $\text{H}_2$ Evolution In Vitro with Natural Components

Coupling the photosynthetic system with a hydrogenase in vitro causes the light-driven liberation of  $\text{O}_2$  and  $\text{H}_2$ . Irradiation of a multicomponent system containing a freshly isolated *Chenopodium album* chloroplast, ferredoxin, and *C. pasteurianum* I [FeFe]-hydrogenase evolved  $\text{H}_2$  at a rate of  $96 \mu\text{mol H}_2 (\text{mg chlorophyll})^{-1} \text{h}^{-1}$  at  $25^\circ\text{C}$ .<sup>[64]</sup> However, the fragile nature of the photosystem and the accumulation of  $\text{O}_2$  in this process results in a fast depletion of  $\text{H}_2$  production. A system consisting of spinach grana,  $\text{NADP}^+$ , FNR,  $\text{NAD}^+$ , and the soluble [NiFe]-hydrogenase from *R. eutropha* H16 was also shown to split water by using visible

light at pH 8 and room temperature over the course of 10 h.<sup>[65]</sup> Photoreduction of hexachloroplatinate(IV),  $[\text{PtCl}_6]^{2-}$ , in a solution containing spinach chloroplasts results in precipitation of metallic Pt on PSI, and continued illumination enables the photosynthetic splitting of water into its elements.<sup>[66]</sup> No electron relay was present in the system, and colloidal Pt was directly in contact with the reducing end of photosystem I in such a way that electron flow occurred across the interface between the biological membrane and the metal colloid.

## Solar $\text{H}_2$ Evolution with Hydrogenases in Solution

$\text{H}_2$  is readily evolved and assayed in the laboratory by a chemical multicomponent system consisting of a hydrogenase, a soluble redox mediator, and a source of low-potential electrons. The last can either (1) be provided by a reducing agent (e.g., dithionite,  $\text{Na}_2\text{S}_2\text{O}_4$ ) or (2) be photocatalytically generated by a photosensitizer (Figure 7). A suitable redox mediator is crucial for electron storage and as an electron-transfer reagent to the enzyme for  $\text{H}_2$  evolution. The excited-state reduction potential ( $E^*$ ) of the photosensitizer must be more negative than the pH-dependent  $\text{H}^+/\text{H}_2$  reduction potential, and the potential of the redox mediator must lie between  $E^*$  of the photosensitizer and the  $\text{H}^+/\text{H}_2$  potential.<sup>[67]</sup>

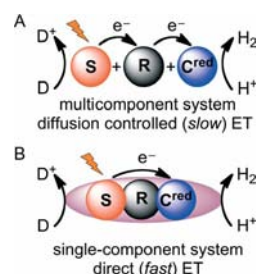


Figure 7. Classification of (A) a multicomponent and (B) a single-component system. The electron relay, R, in B links the photosensitizer, S, directly to the proton-reduction catalyst,  $\text{C}^{\text{red}}$ .

## Diffusion-Controlled Systems

Chloroplasts and ferredoxin can be replaced by a chlorophyll-inspired photosensitizer based on Zn porphyrin and Cyt- $c_3$ , respectively. Cyt- $c$  is a natural electron carrier for periplasmic hydrogenases (see above), and it is suitable as an electron mediator in a multicomponent system with  $\text{ZnPPS}_3$  (Zinc *meso*-tetraphenylporphyrintrisulfonic acid) and membrane-bound [NiFe]-hydrogenase from *Desulfovibrio vulgaris* Miyazaki F in the presence of a sacrificial electron donor (triethanolamine).<sup>[68]</sup> A system consisting of  $[\text{Ru}(\text{bipyridine})_3]^{2+}$  or  $\text{ZnPPS}_3$ , bipyridinium chloride (methyl viologen,  $\text{MV}^{2+}$ ) as redox mediator, and *D. vulgaris* Miyazaki F [NiFe]-MBH was extensively studied.<sup>[69]</sup> Addition of Cyt- $c_3$  to the latter system results in reductive quenching of Cyt- $c_3$  by  $\text{MV}^+$  and accelerated electron trans-



fer to *D. vulgaris* [NiFe]-MBH via the natural redox partner of the enzyme.<sup>[70]</sup> Photoinduced H<sub>2</sub> evolution is also observed upon irradiation of a Cyt-c<sub>3</sub>–viologen–ruthenium(II) triad complex and *D. vulgaris* Miyazaki F [NiFe]-MBH at pH 7.4 in an electron-donating buffer medium.<sup>[71]</sup>

Photocatalytic H<sub>2</sub> production activity does not solely depend on the hydrogenase activity, but also on the other components of the photosystem. Common photosensitizers are [Ru(bipyridine)<sub>3</sub>]<sup>3+/2+</sup> complexes ( $\lambda_{\text{max}} \approx 450$  nm,  $E^* = -0.86$  V vs. NHE)<sup>[72]</sup> or porphyrinoid complexes ( $\lambda_{\text{max}} \approx 500$ –700 nm),<sup>[73]</sup> all of which absorb in the visible region of the solar spectrum to form a relatively long-lived excited state. The redox potential of a redox mediator, such as bipyridinium salts, lies in the range between  $-0.8$  and  $-0.4$  V vs. NHE, which is between  $E^*$  of the photosensitizer and the H<sup>+</sup>/H<sub>2</sub> reduction potential. If the potential of the redox mediator becomes more negative, the driving force for quenching the excited photosensitizer decreases, but the thermodynamics become more favorable for H<sub>2</sub> production.

The stability of the photosensitizer and redox mediator are also important. For example, bipyridyl ligands coordinated to ruthenium(III) (formed in the photocatalytic cycle) are susceptible to nucleophilic attack (e.g., in alkaline aqueous solution by hydroxide ions). Photodecomposition (bleaching) of ruthenium bipyridyl complexes is initiated either by pseudobase formation (breaking of aromaticity by covalent addition of hydroxide to coordinated bipyridyl ligand) or nucleophilic attack of hydroxide at the ruthenium metal center.<sup>[74]</sup>

A major drawback of the described homogeneous, multi-component system for H<sub>2</sub> evolution is that the electron transfer is single and diffusion-limited, and that aeration of the solution leads to immediate quenching of the reduced electron mediator by O<sub>2</sub>. To overcome these limitations, direct electron-transfer-mediated systems with directly linked chromophore–hydrogenase complexes are under development (Figure 7).

### Direct Intermolecular Electron Transfer

Although electron transfer from chemically or photoreduced spinach PSI to free *C. pasteurianum* [NiFe]-hydrogenase I and II occurs directly (in the absence of mediators) in vitro, presumably via the terminal electron acceptor of PSI (F<sub>A</sub>/F<sub>B</sub> in PsaC),<sup>[75]</sup> the direct coupling of a hydrogenase to photosystem I via a molecular or protein wire has emerged as a strategy to promote fast electron transfer.<sup>[76]</sup> A molecular wire of 1,6-hexanedithiol was utilized to link mutated PSI and a [FeFe]-hydrogenase. PSI, which was rebuilt by using the C13S/C33S variant of PsaC, was connected with 1,6-hexanedithiol to the C98G variant of *C. acetobutylicum* [FeFe]-H<sub>2</sub>A or the C225G variant of *C. reinhardtii* [FeFe]-H<sub>2</sub>A, which have a mutated, open-coordination-site distal FeS cluster. Cyt-c<sub>6</sub> and ascorbate were added to act as electron donor to PSI. The construct produces H<sub>2</sub> at a rate of approximately 0.14 mol H<sub>2</sub> (mol hydrogenase)<sup>−1</sup> s<sup>−1</sup> during irradiation (Figure 8).<sup>[76]</sup>

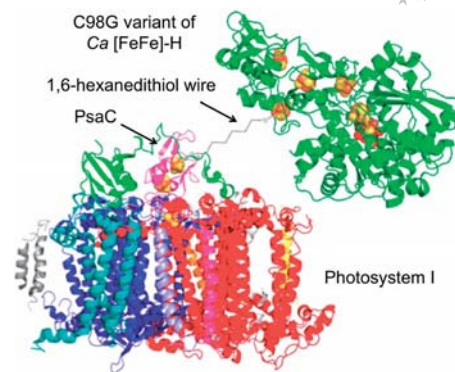


Figure 8. Covalent linkage of PSI to *C. acetobutylicum* [FeFe]-hydrogenase via a 1,6-hexanedithiol wire, which is not drawn to scale for clarity. Reprinted with permission of the American Chemical Society from ref.<sup>[76]</sup>

*R. eutropha* [NiFe]-MBH was coupled to the electron-acceptor side of PSI from cyanobacterial *Synechocystis* PCC 6803 or *Thermosynechococcus elongatus* via its electron-accepting subunit PsaE.<sup>[77]</sup> First, a hydrogenase–PsaE fusion protein was constructed by substituting the membrane anchor domain in the small subunit of *R. eutropha* [NiFe]-MBH by a Gly–Gly linker peptide, which was then fused to PsaE. The purified hydrogenase–PsaE complex showed almost fully remaining wild-type activity. Then, spontaneous association of the hydrogenase–PsaE fusion protein with the PsaE-free PSI generated the hydrogenase–PSI complex, which produced 0.58  $\mu\text{mol H}_2$  (mg chlorophyll)<sup>−1</sup> h<sup>−1</sup> in the presence of ascorbate and TBDB (*N,N,N',N'*-tetramethyl-*p*-phenylenediamine) as electron donors.<sup>[77b]</sup> Irradiation of the immobilized *R. eutropha* [NiFe]-MBH–PsaE–PSI complex on a gold electrode poised at  $-90$  mV vs. NHE in the presence of the redox mediator *N*-methylphenazonium methyl sulfate (PMS; electron donor for P700 in PSI) was also reported to yield H<sub>2</sub>.<sup>[78]</sup>

### Hydrogenases on Solid State Support

Attachment of an electroactive hydrogenase to a conducting surface allows (1) the study of the inherent properties of the enzyme under potential control and different conditions by a suite of electrochemical techniques, (2) acceleration of the diffusion-based step and multielectron transfer at the protein/surface interface, and (3) assembly of heterogeneous catalytic systems for the (photo)electrolysis of water.

### Hydrogenases on Electrodes

Information from protein film electrochemistry (PFE) is crucial to select a suitable enzyme on a specific substrate for a particular application.<sup>[13,26]</sup> Predominantly carbon-based electrodes are used in PFE, in particular the PGE electrode,<sup>[79]</sup> but also carbon felt<sup>[80]</sup> and more recently nanotube<sup>[81]</sup> electrodes have been employed. [FeFe]- and [NiFe]-hydrogenases have also been attached to Au surfaces with a self-assembled monolayer of carboxy- or amino-terminated

mercaptans, respectively, to record surface-enhanced IR absorption (SEIRA) spectra of immobilized hydrogenase.<sup>[82]</sup> Cyanide and carbon monoxide stretching modes give unique and strong marker bands for the active site and allow the investigation of the different states of the enzyme.

A drawback of adsorbing enzymes on a carbon-based electrode is often their poor electrocatalytic coverage and stability. Covalent immobilization of a *D. gigas* [NiFe]-hydrogenase can be achieved by linking the glutamate residues around the distal FeS site of the enzyme to an amine-modified PGE or multiwalled carbon nanotube electrode by the formation of an amide bond (Figure 9).<sup>[83]</sup> The orientation of the enzyme during attachment is controlled by the pH value of the solution through electrostatic interaction with the electrode. The distal FeS cluster of the enzyme is embedded in the negative region of the enzyme dipole (see before), which is attracted by Coulomb forces to the positively charged ammonium groups at the electrode surface, thereby allowing for site-specific covalent attachment of the hydrogenase. Approximately 90% of the initial activity of the enzyme remained after one week of continuous measurement in an H<sub>2</sub> atmosphere at room temperature.<sup>[83]</sup>

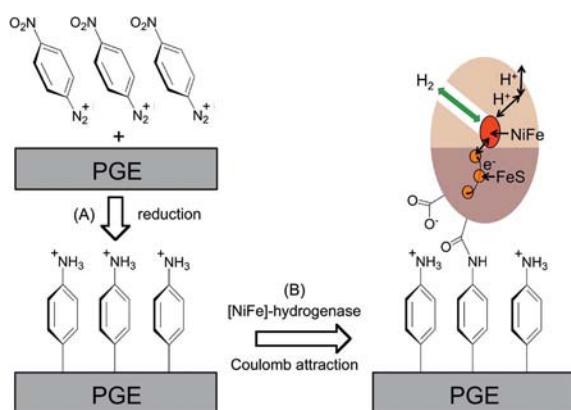


Figure 9. (A) Functionalization of a PGE surface by electrochemical reduction of a nitrophenyldiazonium salt, resulting in a monolayer of phenylamine-functionalized graphite. (B) Covalent grafting of *D. gigas* [NiFe]-hydrogenase to an amine-modified PGE electrode through an amide bond. The pK<sub>a</sub> of the amine is approximately 6.9, and the solution has pH 6.<sup>[83a]</sup>

Even though graphite lacks useful photocatalytic properties, it can be used as electrode material in a photoelectrochemical device. *C. acetobutylicum* [FeFe]-HydA shows a high proton-reduction current (40% of that obtained at a Pt electrode with the same electrode area) when immobilized on a carbon felt (high-surface-area web of low-cost amorphous carbon fibers) electrode and used as the cathode in a photoelectrochemical enzyme fuel cell fitted with a dye-sensitized TiO<sub>2</sub> nanoparticle photoanode and a proton exchange membrane (Figure 10). Illumination of the porphyrin-sensitized TiO<sub>2</sub> nanoparticle photoanode results in photosensitizer excitation and electron transfer to the TiO<sub>2</sub> conduction band (CB). The oxidized radical porphyrin is recovered by oxidation of NADH, regenerating the ground-

state porphyrin. CB electrons are transferred via an external circuit to the hydrogenase-modified PGE cathode, where proton reduction occurs (Figure 6B).<sup>[80,84]</sup>

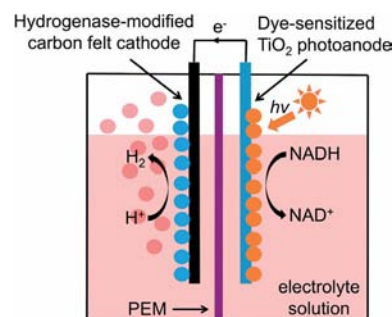


Figure 10. Schematic diagram of a photoelectrochemical enzyme-fuel cell. A porphyrin-based dye is excited by visible light and injects an electron into the conduction band of TiO<sub>2</sub>. The electron reaches the hydrogenase cathode via an external electrical circuit to reduce protons. The oxidized dye is regenerated by the sacrificial electron donor NADH.<sup>[80]</sup>

### Hydrogenases on Particles

Hydrogenases can be adsorbed on particles, and they were shown to catalyze H<sub>2</sub> production or oxidation when coupled with a suitable complementary enzyme redox partner. The direct adsorption of *A. vinosum* [NiFe]-hydrogenase and nitrate reductase from *E. coli* NarGHI (or fumarate reductase from *E. coli* FrdAB) on graphite platelets in the presence of sodium nitrate (or sodium fumarate) in H<sub>2</sub>-flushed buffer results in oxidation of H<sub>2</sub> and production of nitrite (or succinate).<sup>[85]</sup> The water-gas shift reaction [Equation (2)] was catalyzed with quantitative consumption of CO at pH 6 and room temperature when *E. coli* [NiFe]-Hyd2 and [Ni<sub>4</sub>Fe]-carbon monoxide dehydrogenase from *Carboxydotherrmus hydrogenoformans* were co-attached on a graphite particle.<sup>[86]</sup>

Nanoparticles can serve as semi-heterogeneous supports, as they can be readily dispersed in solvents with their high surface area.<sup>[87]</sup> The photocatalytic properties of the semi-conductor TiO<sub>2</sub> have been widely recognized for decades,<sup>[88]</sup> and a photoinduced charge-separated state can be coupled to fuel-forming redox reactions.<sup>[89]</sup> The TiO<sub>2</sub> CB potential is more negative than that of the H<sup>+</sup>/H<sub>2</sub> redox couple, allowing for the reduction of protons to evolve H<sub>2</sub> in the presence of a suitable catalyst. Early reports demonstrated that H<sub>2</sub> evolves from water when TiO<sub>2</sub> nanoparticles are dispersed in the presence of a sacrificial electron donor, a redox mediator (methyl viologen), and an isolated hydrogenase,<sup>[90]</sup> or even when whole bacterial cells from *Clostridium butyricum* are used.<sup>[91]</sup> Direct electron transfer (in the absence of a soluble redox mediator) between TiO<sub>2</sub> and a hydrogenase was observed for a [NiFe]-hydrogenase from *C. pasteurianum*, *D. desulfuricans* Norway and *D. baculatus* 9974,<sup>[92]</sup> and the purple sulfur phototrophic bacterium *Thiocapsa roseopersicina*.<sup>[93]</sup> In these systems, aqueous dispersions of TiO<sub>2</sub> powder and a hydrogenase yielded H<sub>2</sub> upon UV band gap irradiation of TiO<sub>2</sub> (λ < 380 nm) in a sacrificial buffer medium.



Although  $\text{TiO}_2$  is the prototypical semiconducting photocatalyst,<sup>[94]</sup> alternative photocatalysts with improved properties are being investigated.<sup>[95]</sup> Direct photoinduced electron transfer from a CdTe nanocrystal to *C. acetobutylicum* [FeFe]-HydA yields 25 mol  $\text{H}_2$  (mol hydrogenase)<sup>-1</sup> s<sup>-1</sup> and a quantum yield of 1.8% under standard sunlight (AM 1.5 irradiation) in the presence of ascorbic acid.<sup>[96]</sup> Irradiating aqueous suspensions of CdS coupled to [NiFe]-hydrogenase from *T. roseopersicina* in the presence of formate results in the production of metallic Cd and  $\text{H}_2$ , CO and  $\text{CO}_2$ .  $\text{Cd}^0$  was suggested to activate direct CB electron transfer to the hydrogenase.<sup>[97]</sup>

Protein film electrochemical studies with various hydrogenases attached on a thin film nanoparticle  $\text{TiO}_2$ -ITO (ITO: indium-doped tin oxide) electrode lead to the selection of a *titaniophilic* hydrogenase – *D. baculatum* [NiFeSe]-hydrogenase. The electrochemical response of this hydrogenase showed high electrocatalytic activity for  $\text{H}_2$  production and high stability at neutral pH, a feature ascribed to the remarkable biocompatibility and hydrophilicity of  $\text{TiO}_2$ . About 80% of the electrocatalytic activity was retained after 48 h and 50% after storage for one month in the electrolyte solution at room temperature under  $\text{N}_2$ .<sup>[98]</sup> Strong interactions of  $\text{TiO}_2$  with several amino acids<sup>[99]</sup> as well as other enzymes are well known.<sup>[100]</sup> Particularly strong interactions have been reported for the acidic amino acids aspartic and glutamic acid with  $\text{TiO}_2$ ,<sup>[101]</sup> and the latter binds to  $\text{TiO}_2$  even in alkaline medium (pH 8).<sup>[102]</sup> *D.*

*baculatum* [NiFeSe]-hydrogenase contains a glutamate- and aspartate-rich surface environment around the distal [4Fe4S] cluster, Glu260, Glu234, Glu224, Glu221, Asp218, Asp215, Glu209, Asp205 providing strong potential anchors for the enzyme to  $\text{TiO}_2$  (Figure 4). A dominating chemical bond rather than weak (repulsive) electrostatic interactions are presumably responsible for the stable attachment of *Db* [NiFeSe]-hydrogenase to  $\text{TiO}_2$ .

To overcome the limitation of having to use only the UV spectrum of solar light and to avoid the formation of reactive (highly oxidizing) electron holes in the valence band of  $\text{TiO}_2$  during UV band gap irradiation, a ruthenium photosensitizer (RuP) was co-attached with *D. baculatum* [NiFeSe]-hydrogenase to  $\text{TiO}_2$  (Figure 11).<sup>[103]</sup> Ruthenium dyes attached to  $\text{TiO}_2$  allow for ultrafast electron injection into the CB of  $\text{TiO}_2$ , a concept that is exploited in dye-sensitized solar cells.<sup>[104]</sup> The assembled photocatalytic system consisting of *Db* [NiFeSe]-H and ruthenium photosensitizer on  $\text{TiO}_2$  produces  $\text{H}_2$  efficiently at a rate of 50 mol  $\text{H}_2$  (mol hydrogenase)<sup>-1</sup> s<sup>-1</sup> in the presence of a sacrificial electron donor (triethanolamine) over several hours. The photosensitizer operates as an artificial light-harvesting antenna system, which absorbs light and provides the CB of  $\text{TiO}_2$  with an excess of electrons, which  $\text{TiO}_2$  provides *as needed* to the enzyme (Figures 6B and 11). Attachment of a photosensitizer and a catalyst on a particle not only allows direct multi-electron transfer, but also makes it possible to vary the ratio of the attached components to optimize the photocatalytic efficiency.

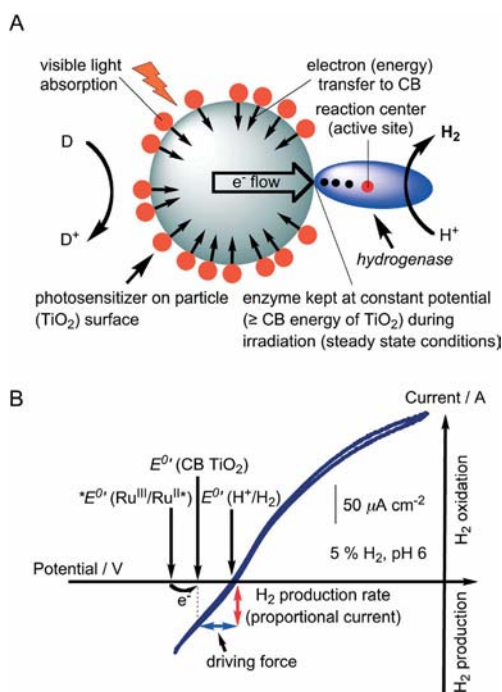


Figure 11. Concept of light-driven  $\text{H}_2$  production with a hydrogenase-modified dye-sensitized  $\text{TiO}_2$  nanoparticle in the presence of a sacrificial electron donor (D).<sup>[103]</sup> An antenna system of ruthenium photosensitizers harvests visible light, injects electrons into the CB of  $\text{TiO}_2$ , and the resulting constant flow of electrons (steady state conditions) produces a low potential at the hydrogenase. (A) Schematic and (B) electrochemical representation.

## Conclusions

Much information is now available on photobiological water splitting and recent strategies to select and utilize hydrogenases in photocatalytic  $\text{H}_2$  production systems have been summarized. Different hydrogenases with their subtle changes in the hydrogenase active site or protein environment exhibit very distinct properties. The technological application of hydrogenases is currently prohibited by the high cost of isolation and purification, voluminous footprint (low density) and fragility (in particular  $\text{O}_2$ -sensitivity and instability). However, hydrogenases, and, in particular, their active sites, offer an interesting motif for the synthesis of lower-cost catalysts to replace expensive Pt catalysts; a prerequisite for solar  $\text{H}_2$  technology to become economically viable. The 3d-metal active site of a hydrogenase stands as a benchmark for kinetic and thermodynamic efficiency and has a high inspirational value for the preparation of small-molecule catalysts assembled from abundant raw materials. Many significant advances have been made in recent years to improve the efficiency of small-molecule catalysts. One noteworthy example is the covalent attachment of a Ni bis(diphosphane)-based functional hydrogenase mimic on a multiwalled carbon nanotube. These large-area electrodes exhibit only a small overpotential (20 mV) for  $\text{H}_2$  cycling and show current densities similar to those observed for hydrogenase-based materials.<sup>[105]</sup> I am confident that, with

the fast progress in the mature hydrogenase field, synthetic chemist will soon challenge the efficiency of the enzyme and implement inexpensive catalysts into photoelectrochemical devices for solar H<sub>2</sub> production.

## Acknowledgments

I am grateful to Prof. Fraser A. Armstrong and his group for help and support over the last couple of years. Prof. David Collison is acknowledged for helpful discussions and Dr. Alison Parkin and Dr. Gabrielle Goldet for providing the Pymol representation and the raw data used in Figures 2 and 5, respectively. The Engineering and Physical Sciences Research Council (EP/H00338X/1) and The University of Manchester supported this work.

- [1] a) N. S. Lewis, *Science* **2007**, *315*, 798–801; b) V. Balzani, A. Credi, M. Venturi, *ChemSusChem* **2008**, *1*, 26–58; c) P. D. Tran, V. Artero, M. Fontecave, *Energy Environ. Sci.* **2010**, *3*, 727–747.
- [2] a) R. M. Navarro, M. A. Peña, J. L. G. Fierro, *Chem. Rev.* **2007**, *107*, 3952–3991; b) J. H. Lunsford, *Catal. Today* **2000**, *63*, 165–174.
- [3] a) N. S. Lewis, D. G. Nocera, *Proc. Natl. Acad. Sci. USA* **2006**, *103*, 15729–15735; b) G. Centi, S. Perathoner, *ChemSusChem* **2010**, *3*, 195–208; c) D. Gust, T. A. Moore, A. L. Moore, *Acc. Chem. Res.* **2009**, *42*, 1890–1898; d) A. Magnuson, M. Anderlund, O. Johansson, P. Lindblad, R. Lomoth, T. Polivka, S. Ott, K. Stensjö, S. Styring, V. Sundström, L. Hammarström, *Acc. Chem. Res.* **2009**, *42*, 1899–1909; e) N. Armaroli, V. Balzani, *Angew. Chem. Int. Ed.* **2007**, *46*, 52–66.
- [4] a) D. R. Palo, R. A. Dagle, J. D. Holladay, *Chem. Rev.* **2007**, *107*, 3992–4021; b) S. Friedle, E. Reisner, S. J. Lippard, *Chem. Soc. Rev.* **2010**, *39*, 2768–2779.
- [5] J. L. Casci, C. M. Lok, M. D. Shannon, *Catal. Today* **2009**, *145*, 38–44.
- [6] a) I. McConnell, G. Li, G. W. Brudvig, *Chem. Biol.* **2010**, *17*, 434–447; b) P. C. Hallenbeck, J. R. Benemann, *Int. J. Hydrogen Energy* **2002**, *27*, 1185–1193.
- [7] a) D. G. Nocera, *Inorg. Chem.* **2009**, *48*, 10001–10017; b) A. Kudo, Y. Miseki, *Chem. Soc. Rev.* **2009**, *38*, 253–278.
- [8] W. Lubitz, E. J. Reijerse, J. Messinger, *Energy Environ. Sci.* **2008**, *1*, 15–31.
- [9] J. C. Fontecilla-Camps, P. Amara, C. Cavazza, Y. Nicolet, A. Volbeda, *Nature* **2009**, *460*, 814–822.
- [10] J. C. Fontecilla-Camps, A. Volbeda, C. Cavazza, Y. Nicolet, *Chem. Rev.* **2007**, *107*, 4273–4303.
- [11] a) P. M. Vignais, B. Billoud, *Chem. Rev.* **2007**, *107*, 4206–4272; b) P. M. Vignais, B. Billoud, J. Meyer, *FEMS Microbiol. Rev.* **2001**, *25*, 455–501.
- [12] a) H. Ogata, W. Lubitz, Y. Higuchi, *Dalton Trans.* **2009**, 7577–7587; b) W. Lubitz, E. Reijerse, M. van Gastel, *Chem. Rev.* **2007**, *107*, 4331–4365; c) A. L. de Lacey, V. M. Fernández, *Chem. Rev.* **2007**, *107*, 4304–4330.
- [13] K. A. Vincent, A. Parkin, F. A. Armstrong, *Chem. Rev.* **2007**, *107*, 4366–4413.
- [14] S. Shima, R. K. Thauer, *Chem. Rec.* **2007**, *7*, 37–46.
- [15] a) S. Shima, O. Pilak, S. Vogt, M. Schick, M. S. Stagni, W. Meyer-Klaucke, E. Warkentin, R. K. Thauer, U. Ermler, *Science* **2008**, *321*, 572–575; b) T. Hiromoto, E. Warkentin, J. Moll, U. Ermler, S. Shima, *Angew. Chem. Int. Ed.* **2009**, *48*, 6457–6460; c) T. Hiromoto, K. Ataka, O. Pilak, S. Vogt, M. S. Stagni, W. Meyer-Klaucke, E. Warkentin, R. K. Thauer, S. Shima, U. Ermler, *FEBS Lett.* **2009**, *583*, 585–590.
- [16] S. Vogt, E. J. Lyon, S. Shima, R. K. Thauer, *J. Biol. Inorg. Chem.* **2008**, *13*, 97–106.
- [17] a) J. W. Peters, W. N. Lanzilotta, B. J. Lemon, L. C. Seefeldt, *Science* **1998**, *282*, 1853–1858; b) A. S. Pandey, T. V. Harris, L. J. Giles, J. W. Peters, R. K. Szilagyi, *J. Am. Chem. Soc.* **2008**, *130*, 4533–4540.
- [18] Y. Nicolet, C. Piras, P. Legrand, C. E. Hatchikian, J. C. Fontecilla-Camps, *Structure* **1999**, *7*, 13–23.
- [19] D. W. Mulder, E. S. Boyd, R. Sarma, R. K. Lange, J. A. Endrizzi, J. B. Broderick, J. W. Peters, *Nature* **2010**, *465*, 248–252.
- [20] Y. Nicolet, B. J. Lemon, J. C. Fontecilla-Camps, J. W. Peters, *Trends Biochem. Sci.* **2000**, *25*, 138–143.
- [21] a) A. Silakov, B. Wenk, E. Reijerse, W. Lubitz, *Phys. Chem. Chem. Phys.* **2009**, *11*, 6592–6599; b) B. E. Barton, M. T. Olsen, T. B. Rauchfuss, *J. Am. Chem. Soc.* **2008**, *130*, 16834–16835.
- [22] a) L. Florin, A. Tsokoglou, T. Happe, *J. Biol. Chem.* **2001**, *276*, 6125–6132; b) S. Stripp, O. Sanganas, T. Happe, M. Haumann, *Biochemistry* **2009**, *48*, 5042–5049.
- [23] a) A. Volbeda, M.-H. Charon, C. Piras, E. C. Hatchikian, M. Frey, J. C. Fontecilla-Camps, *Nature* **1995**, *373*, 580–587; b) Y. Montet, P. Amara, A. Volbeda, X. Vernede, E. C. Hatchikian, M. J. Field, M. Frey, J. C. Fontecilla-Camps, *Nat. Struct. Biol.* **1997**, *4*, 523–526; c) Y. Higuchi, T. Yagi, N. Yasuoka, *Structure* **1997**, *5*, 1671–1680; d) P. M. Matias, C. M. Soares, L. M. Saraiva, R. Coelho, J. Morais, J. Le Gall, M. A. Carrondo, *J. Biol. Inorg. Chem.* **2001**, *6*, 63–81; e) E. Garcin, X. Vernede, E. C. Hatchikian, A. Volbeda, M. Frey, J. C. Fontecilla-Camps, *Structure* **1999**, *7*, 557–566; f) A. Volbeda, L. Martin, C. Cavazza, M. Matho, B. W. Faber, W. Roseboom, S. P. J. Albracht, E. Garcin, M. Rousset, J. C. Fontecilla-Camps, *J. Biol. Inorg. Chem.* **2005**, *10*, 239–249.
- [24] P. Kellers, H. Ogata, W. Lubitz, *Acta Crystallogr., Sect. F: Struct. Biol. Cryst. Commun.* **2008**, *64*, 719–722.
- [25] a) F. Leroux, S. Dementin, B. Burlat, L. Cournac, A. Volbeda, S. Champ, L. Martin, B. Guigliarelli, P. Bertrand, J. Fontecilla-Camps, M. Rousset, C. Léger, *Proc. Natl. Acad. Sci. USA* **2008**, *105*, 11188–11193; b) P.-P. Liebgott, F. Leroux, B. Burlat, S. Dementin, C. Baffert, T. Lautier, V. Fourmond, P. Ceccaldi, C. Cavazza, I. Meynial-Salles, P. Soucaille, J. C. Fontecilla-Camps, B. Guigliarelli, P. Bertrand, M. Rousset, C. Leger, *Nat. Chem. Biol.* **2010**, *6*, 63–70.
- [26] C. Léger, P. Bertrand, *Chem. Rev.* **2008**, *108*, 2379–2438.
- [27] A. K. Jones, E. Sillery, S. P. J. Albracht, F. A. Armstrong, *Chem. Commun.* **2002**, 866–867.
- [28] F. A. Armstrong, N. A. Belsey, J. A. Cracknell, G. Goldet, A. Parkin, E. Reisner, K. A. Vincent, A. F. Wait, *Chem. Soc. Rev.* **2009**, *38*, 36–51.
- [29] a) K. A. Vincent, J. A. Cracknell, O. Lenz, I. Zebger, B. Friedrich, F. A. Armstrong, *Proc. Natl. Acad. Sci. USA* **2005**, *102*, 16951–16954; b) K. A. Vincent, J. A. Cracknell, J. R. Clark, M. Ludwig, O. Lenz, B. Friedrich, F. A. Armstrong, *Chem. Commun.* **2006**, 5033–5035; c) J. A. Cracknell, K. A. Vincent, F. A. Armstrong, *Chem. Rev.* **2008**, *108*, 2439–2461; d) A. F. Wait, A. Parkin, G. M. Morley, L. dos Santos, F. A. Armstrong, *J. Phys. Chem. C* **2010**, *114*, 12003–12009.
- [30] J. A. Cracknell, A. F. Wait, O. Lenz, B. Friedrich, F. A. Armstrong, *Proc. Natl. Acad. Sci. USA* **2009**, *106*, 20681–20686.
- [31] a) M. van Gastel, M. Stein, M. Brecht, O. Schröder, F. Lendzian, R. Bittl, H. Ogata, Y. Higuchi, W. Lubitz, *J. Biol. Inorg. Chem.* **2006**, *11*, 41–51; b) V. M. Fernández, E. C. Hatchikian, D. S. Patil, R. Cammack, *Biochim. Biophys. Acta* **1986**, *883*, 145–154.
- [32] K. A. Vincent, A. Parkin, O. Lenz, S. P. J. Albracht, J. C. Fontecilla-Camps, R. Cammack, B. Friedrich, F. A. Armstrong, *J. Am. Chem. Soc.* **2005**, *127*, 18179–18189.
- [33] O. Lenz, M. Ludwig, T. Schubert, I. Bürschel, S. Ganskow, T. Goris, A. Schwarze, B. Friedrich, *ChemPhysChem* **2010**, *11*, 1107–1119.
- [34] S. Dementin, F. Leroux, L. Cournac, A. L. de Lacey, A. Volbeda, C. Léger, B. Burlat, N. Martinez, S. Champ, L. Martin, O. Sanganas, M. Haumann, V. M. Fernández, B. Guigliarelli, J. C. Fontecilla-Camps, M. Rousset, *J. Am. Chem. Soc.* **2009**, *131*, 10156–10164.

- [35] P. M. Vignais, A. Colbeau, *Curr. Issues Mol. Biol.* **2004**, *6*, 159–188.
- [36] P. M. Matias, A. V. Coelho, F. M. A. Valente, D. Plácido, J. Le Gall, A. V. Xavier, I. A. C. Pereira, M. A. Carrondo, *J. Biol. Chem.* **2002**, *277*, 47907–47916.
- [37] a) M. Winkler, S. Kuhlert, M. Hippler, T. Happe, *J. Biol. Chem.* **2009**, *284*, 36620–36627; b) C. H. Chang, P. W. King, M. L. Ghirardi, K. Kim, *Biophys. J.* **2007**, *93*, 3034–3045.
- [38] a) G. Goldet, C. Brandmayr, S. T. Stripp, T. Happe, C. Cavazza, J. C. Fontecilla-Camps, F. A. Armstrong, *J. Am. Chem. Soc.* **2009**, *131*, 14979–14989; b) S. T. Stripp, G. Goldet, C. Brandmayr, O. Sanganas, K. A. Vincent, M. Haumann, F. A. Armstrong, T. Happe, *Proc. Natl. Acad. Sci. USA* **2009**, *106*, 17331–17336.
- [39] S. T. Stripp, T. Happe, *Dalton Trans.* **2009**, 9960–9969.
- [40] P. W. King, M. C. Posewitz, M. L. Ghirardi, M. Seibert, *J. Bacteriol.* **2006**, *188*, 2163–2172.
- [41] T. Burgdorf, O. Lenz, T. Buhrke, E. van der Linden, A. K. Jones, S. P. J. Albracht, B. Friedrich, *J. Mol. Microbiol. Biotechnol.* **2005**, *10*, 181–196.
- [42] G. Goldet, A. F. Wait, J. A. Cracknell, K. A. Vincent, M. Ludwig, O. Lenz, B. Friedrich, F. A. Armstrong, *J. Am. Chem. Soc.* **2008**, *130*, 11106–11113.
- [43] R. Huber, K. O. Stetter in *Methods Enzymol.*, Vol. 330 (Eds.: M. W. W. Adams, R. M. Kelly), Academic Press, New York, **2001**, pp. 11–24.
- [44] M.-E. Pandelia, V. Fourmond, P. Tron-Infossi, E. Lojou, P. Bertrand, C. Léger, M.-T. Giudici-Orticoni, W. Lubitz, *J. Am. Chem. Soc.* **2010**, *132*, 6991–7004.
- [45] M. J. Lukey, A. Parkin, M. M. Roessler, B. J. Murphy, J. Harmer, T. Palmer, F. Sargent, F. A. Armstrong, *J. Biol. Chem.* **2010**, *285*, 3928–3938.
- [46] G. Sawers, *Antonie van Leeuwenhoek* **1994**, *66*, 57–88.
- [47] a) E. Lojou, X. Luo, M. Brugna, N. Candoni, S. Dementin, M. T. Giudici-Orticoni, *J. Biol. Inorg. Chem.* **2008**, *13*, 1157–1167; b) P. Infossi, E. Lojou, J.-P. Chauvin, G. Herbet, M. Brugna, M.-T. Giudici-Orticoni, *Int. J. Hydrogen Energy* **2010**, *35*, 10778–10789.
- [48] a) M. Teixeira, G. Fauque, I. Moura, P. A. Lepinat, Y. Berlier, B. Prickril, H. D. Peck Jr., A. V. Xavier, J. Le Gall, J. J. G. Moura, *Eur. J. Biochem.* **1987**, *167*, 47–58; b) F. M. A. Valente, A. S. F. Oliveira, N. Gnadt, I. Pacheco, A. V. Coelho, A. V. Xavier, M. Teixeira, C. M. Soares, I. A. C. Pereira, *J. Biol. Inorg. Chem.* **2005**, *10*, 667–682.
- [49] A. Parkin, G. Goldet, C. Cavazza, J. C. Fontecilla-Camps, F. A. Armstrong, *J. Am. Chem. Soc.* **2008**, *130*, 13410–13416.
- [50] F. M. A. Valente, C. C. Almeida, I. Pacheco, J. Carita, L. M. Saraiva, I. A. C. Pereira, *J. Bacteriol.* **2006**, *188*, 3228–3235.
- [51] A. L. de Lacey, C. Gutiérrez-Sánchez, V. Fernández, I. Pacheco, I. Pereira, *J. Biol. Inorg. Chem.* **2008**, *13*, 1315–1320.
- [52] M. C. Marques, R. Coelho, A. L. de Lacey, I. A. C. Pereira, P. M. Matias, *J. Mol. Biol.* **2010**, *396*, 893–907.
- [53] a) J. Barber, *Nat. Struct. Mol. Biol.* **2001**, *8*, 577–579; b) A. Amunts, O. Drory, N. Nelson, *Nature* **2007**, *447*, 58–63.
- [54] a) K. N. Ferreira, T. M. Iverson, K. Maghlaoui, J. Barber, S. Iwata, *Science* **2004**, *303*, 1831–1838; b) A. Guskov, J. Kern, A. Gabdulkhakov, M. Broser, A. Zouni, W. Saenger, *Nat. Struct. Mol. Biol.* **2009**, *16*, 334–342.
- [55] O. Kruse, J. Rupprecht, J. H. Mussnug, G. C. Dismukes, B. Hankamer, *Photochem. Photobiol. Sci.* **2005**, *4*, 957–970.
- [56] P. Sétif, N. Harris, B. Lagoutte, S. Dotson, S. R. Weinberger, *J. Am. Chem. Soc.* **2010**, *132*, 10620–10622.
- [57] a) M. L. Ghirardi, A. Dubini, J. Yu, P.-C. Maness, *Chem. Soc. Rev.* **2009**, *38*, 52–61; b) A. Melis, T. Happe, *Plant Physiol.* **2001**, *127*, 740–748; c) L. Cournac, G. Guedeney, G. Peltier, P. M. Vignais, *J. Bacteriol.* **2004**, *186*, 1737–1746; d) M. Calusinska, T. Happe, B. Joris, A. Wilmotte, *Microbiol.* **2010**, *156*, 1575–1588; e) A. Melis, T. Happe, *Photosynth. Res.* **2004**, *80*, 401–409.
- [58] a) R. Hedderich, *J. Bioenerg. Biomembr.* **2004**, *36*, 65–75; b) M. L. Ghirardi, M. C. Posewitz, P.-C. Maness, A. Dubini, J. Yu, M. Seibert, *Annu. Rev. Plant Biol.* **2007**, *58*, 71–91.
- [59] A. Hemschemeier, S. Fouchard, L. Cournac, G. Peltier, T. Happe, *Planta* **2008**, *227*, 397–407.
- [60] E. Greenbaum, S. L. Blankinship, J. W. Lee, R. M. Ford, *J. Phys. Chem. B* **2001**, *105*, 3605–3609.
- [61] A. Melis, L. Zhang, M. Forestier, M. L. Ghirardi, M. Seibert, *Plant Physiol.* **2000**, *122*, 127–135.
- [62] V. Chochois, D. Dauvillee, A. Beyly, D. Tolleter, S. Cuine, H. Timpino, S. Ball, L. Cournac, G. Peltier, *Plant Physiol.* **2009**, *151*, 631–640.
- [63] a) L. Zhang, T. Happe, A. Melis, *Planta* **2002**, *214*, 552–561; b) T. K. Antal, T. E. Krendeleve, T. V. Laurinavichene, V. V. Makarova, M. L. Ghirardi, A. B. Rubin, A. A. Tsygankov, M. Seibert, *Biochim. Biophys. Acta Bioenerg.* **2003**, *1607*, 153–160.
- [64] a) J. R. Benemann, J. A. Berenson, N. O. Kaplan, M. D. Kamen, *Proc. Natl. Acad. Sci. USA* **1973**, *70*, 2317–2320; b) K. K. Rao, I. N. Gogotov, D. O. Hall, *Biochimie* **1978**, *60*, 291–296.
- [65] F. Hasumi, T. Yamamoto, I. Okura, *Inorg. Chim. Acta* **1992**, *202*, 1–2.
- [66] E. Greenbaum, *Science* **1985**, *230*, 1373–1375.
- [67] S. Fukuzumi, *Eur. J. Inorg. Chem.* **2008**, 1351–1362.
- [68] I. Okura, M. Takeuchi, S. Kusunoki, S. Aono, *Chem. Lett.* **1982**, *11*, 187–188.
- [69] a) I. Okura, *Coord. Chem. Rev.* **1985**, *68*, 53–99; b) I. Okura, *Biochimie* **1986**, *68*, 189–199.
- [70] T. Hiraishi, T. Kamachi, I. Okura, *J. Photochem. Photobiol., A* **1996**, *101*, 45–47.
- [71] N. Asakura, T. Hiraishi, T. Kamachi, I. Okura, *J. Mol. Catal. A* **2001**, *172*, 1–7.
- [72] A. Juris, V. Balzani, F. Barigelletti, S. Campagna, P. Belser, A. von Zelewsky, *Coord. Chem. Rev.* **1988**, *84*, 85–277.
- [73] K. Lang, J. Mosinger, D. M. Wagnerová, *Coord. Chem. Rev.* **2004**, *248*, 321–350.
- [74] a) J. K. Hurst, *Coord. Chem. Rev.* **2005**, *249*, 313–328; b) J. W. Bunting in *Adv. Heterocycl. Chem.* Vol. 25 (Eds.: A. R. Katritzky, A. J. Boulton), Academic Press, New York, **1980**, pp. 1–82; c) J. A. A. Sagüés, R. D. Gillard, R. J. Lancashire, P. A. Williams, *J. Chem. Soc., Dalton Trans.* **1979**, 193–198; d) P. A. Lay, W. H. F. Sasse, *Inorg. Chem.* **1985**, *24*, 4707–4710.
- [75] H. McTavish, *J. Biochem.* **1998**, *123*, 644–649.
- [76] C. E. Lubner, R. Grimme, D. A. Bryant, J. H. Golbeck, *Biochemistry* **2010**, *49*, 404–414.
- [77] a) M. Ihara, H. Nishihara, K.-S. Yoon, O. Lenz, B. Friedrich, H. Nakamoto, K. Kojima, D. Honma, T. Kamachi, I. Okura, *Photochem. Photobiol.* **2006**, *82*, 676–682; b) A. Schwarze, M. J. Kopczak, M. Roegner, O. Lenz, *Appl. Environ. Microbiol.* **2010**, *76*, 2641–2651.
- [78] H. Krassen, A. Schwarze, B. Friedrich, K. Ataka, O. Lenz, J. Heberle, *ACS Nano* **2009**, *3*, 4055–4061.
- [79] C. F. Blanford, F. A. Armstrong, *J. Solid State Electrochem.* **2006**, *10*, 826–832.
- [80] M. Hambourger, M. Gervaldo, D. Svedruzic, P. W. King, D. Gust, M. Ghirardi, A. L. Moore, T. A. Moore, *J. Am. Chem. Soc.* **2008**, *130*, 2015–2022.
- [81] a) F. J. M. Hoebe, I. Heller, S. P. J. Albracht, C. Dekker, S. G. Lemay, H. A. Heering, *Langmuir* **2008**, *24*, 5925–5931; b) T. J. McDonald, D. Svedruzic, Y.-H. Kim, J. L. Blackburn, S. B. Zhang, P. W. King, M. J. Heben, *Nano Lett.* **2007**, *7*, 3528–3534; c) O. A. Zadovny, A. M. Barrows, N. A. Zorin, J. W. Peters, T. E. Elgren, *J. Mater. Chem.* **2010**, *20*, 1065–1067; d) L. Hu, D. S. Hecht, G. Grüner, *Chem. Rev.* **2010**, *110*, 5790–5844.
- [82] a) H. Krassen, S. Stripp, G. von Abendroth, K. Ataka, T. Happe, J. Heberle, *J. Biotechnol.* **2009**, *142*, 3–9; b) D. Millo, M.-E. Pandelia, T. Utesch, N. Wisitruangsakul, M. A. Mrogin-ski, W. Lubitz, P. Hildebrandt, I. Zebger, *J. Phys. Chem. B* **2009**, *113*, 15344–15351; c) N. Wisitruangsakul, O. Lenz, M. Ludwig, B. Friedrich, F. Lendzian, P. Hildebrandt, I. Zebger, *Angew. Chem. Int. Ed.* **2009**, *48*, 611–613.



- [83] a) O. Rüdiger, J. M. Abad, E. C. Hatchikian, V. M. Fernandez, A. L. de Lacey, *J. Am. Chem. Soc.* **2005**, *127*, 16008–16009; b) M. A. Alonso-Lomillo, O. Rüdiger, A. Maroto-Valiente, M. Velez, I. Rodríguez-Ramos, F. J. Muñoz, V. M. Fernández, A. L. de Lacey, *Nano Lett.* **2007**, *7*, 1603–1608.
- [84] M. Hambourger, G. F. Moore, D. M. Kramer, D. Gust, A. L. Moore, T. A. Moore, *Chem. Soc. Rev.* **2009**, *38*, 25–35.
- [85] K. A. Vincent, X. Li, C. F. Blanford, N. A. Belsey, J. H. Weiner, F. A. Armstrong, *Nat. Chem. Biol.* **2007**, *3*, 761–762.
- [86] O. Lazarus, T. W. Woolerton, A. Parkin, M. J. Lukey, E. Reisner, J. Seravalli, E. Pierce, S. W. Ragsdale, F. Sargent, F. A. Armstrong, *J. Am. Chem. Soc.* **2009**, *131*, 14154–14155.
- [87] A. Schätz, O. Reiser, W. J. Stark, *Chem. Eur. J.* **2010**, *16*, 8950–8967.
- [88] A. Fujishima, K. Honda, *Nature* **1972**, *238*, 37–38.
- [89] H. J. Lewerenz, C. Heine, K. Skorupska, N. Szabo, T. Hannappel, T. Vo-Dinh, S. A. Campbell, H. W. Klemm, A. G. Muñoz, *Energy Environ. Sci.* **2010**, *3*, 748–760.
- [90] a) P. Cuendet, M. Grätzel, K. K. Rao, D. O. Hall, *Photobiophys. Photobiophys.* **1984**, *7*, 331–340; b) P. Cuendet, M. Grätzel, M. L. Pelaprat, *J. Electroanal. Chem.* **1984**, *181*, 173–185.
- [91] A. A. Krasnovsky, V. V. Nikandrov, *FEBS Lett.* **1987**, *219*, 93–96.
- [92] P. Cuendet, K. K. Rao, M. Grätzel, D. O. Hall, *Biochimie* **1986**, *68*, 217–221.
- [93] a) I. N. Gogotov, N. A. Zorin, L. T. Serebryakova, *Int. J. Hydrogen Energy* **1991**, *16*, 393–396; b) V. V. Nikandrov, M. A. Shlyk, N. A. Zorin, I. N. Gogotov, A. A. Krasnovsky, *FEBS Lett.* **1988**, *234*, 111–114.
- [94] a) D. Y. C. Leung, X. Fu, C. Wang, M. Ni, M. K. H. Leung, X. Wang, X. Fu, *ChemSusChem* **2010**, *3*, 681–694; b) X. Chen, S. S. Mao, *Chem. Rev.* **2007**, *107*, 2891–2959.
- [95] M. D. Hernandez-Alonso, F. Fresno, S. Suarez, J. M. Coronado, *Energy Environ. Sci.* **2009**, *2*, 1231–1257.
- [96] K. A. Brown, S. Dayal, X. Ai, G. Rumbles, P. W. King, *J. Am. Chem. Soc.* **2010**, *132*, 9672–9680.
- [97] A. I. Nedoluzhko, I. A. Shumilin, V. V. Nikandrov, *J. Phys. Chem.* **1996**, *100*, 17544–17550.
- [98] E. Reisner, J. C. Fontecilla-Camps, F. A. Armstrong, *Chem. Commun.* **2009**, 550–552.
- [99] T. H. Tran, A. Y. Nosaka, Y. Nosaka, *J. Phys. Chem. B* **2006**, *110*, 25525–25531.
- [100] a) E. Topoglidis, C. J. Campbell, A. E. G. Cass, J. R. Durrant, *Langmuir* **2001**, *17*, 7899–7906; b) E. Topoglidis, A. E. G. Cass, B. O'Regan, J. R. Durrant, *J. Electroanal. Chem.* **2001**, *517*, 20–27; c) E. Topoglidis, E. Palomares, Y. Astuti, A. Green, C. J. Campbell, J. R. Durrant, *Electroanalysis* **2005**, *17*, 1035–1041.
- [101] Z. Paszti, T. Keszthelyi, O. Hakkel, L. Guzzi, *J. Phys.: Condens. Matter* **2008**, *20*, 224014.
- [102] A. D. Roddick-Lanzilotta, A. J. McQuillan, *J. Colloid Interface Sci.* **2000**, *227*, 48–54.
- [103] E. Reisner, D. J. Powell, C. Cavazza, J. C. Fontecilla-Camps, F. A. Armstrong, *J. Am. Chem. Soc.* **2009**, *131*, 18457–18466.
- [104] M. Grätzel, *Inorg. Chem.* **2005**, *44*, 6841–6851.
- [105] A. Le Goff, V. Artero, B. Jousselme, P. D. Tran, N. Guillet, R. Métayé, A. Fihri, S. Palacin, M. Fontecave, *Science* **2009**, *326*, 1384–1387.

Received: September 15, 2010

Published Online: December 3, 2010